FLAME measurements and test-beam analysis

Dawid Pietruch

AGH University of Krakow, Faculty of Physics and Applied Computer Science

pietruch@agh.edu.pl

7.09.2023

Plan of the presentation

Laboratory measurements

Testing board

We have recently received injector board and are at the beginning of the systematic FLAME measurements.

Injected charge: 2.5 - 250 fC
All 128 channels can be activated separately using a jumper.

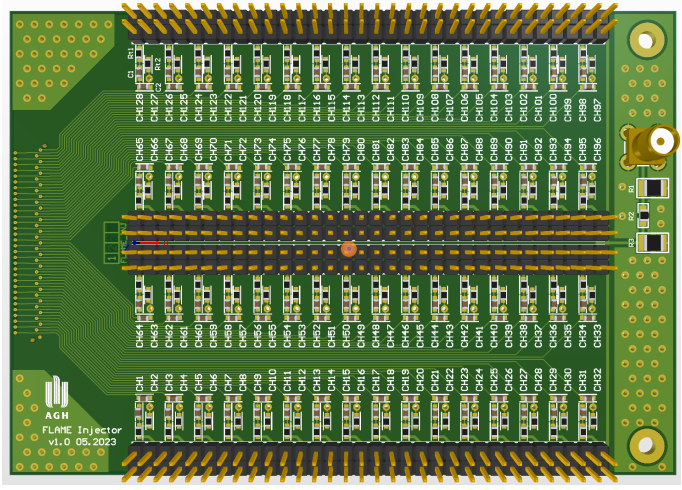

Fig. 1: Testing board visualisation

Preliminary calibration of FLAME readout

All channels were tested by injecting the same charges 48.5, 92.3 and 136.1 fC for three-point linear regression.

The peek-to-peek gain fluctuations between channels are below 3%.

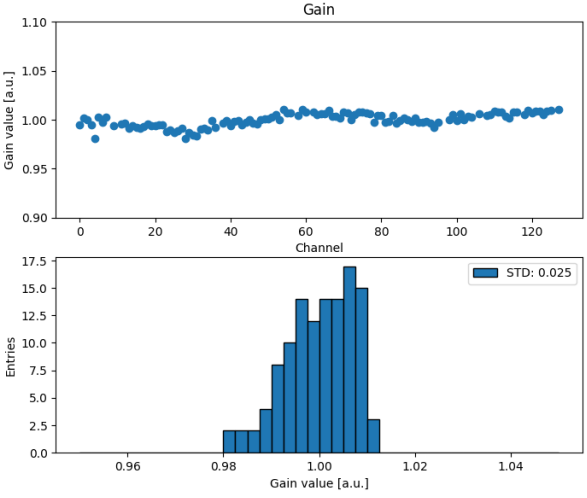

Fig. 2: Preliminary calibration of FLAME readout channels

FLAME pulse shape

Another test was to obtain a detailed pulse shape which was seen from the perspective of the ADC. In this case, the phase of initial pulse from generator ws changed in range 0 - 50 ns by 1 ns.

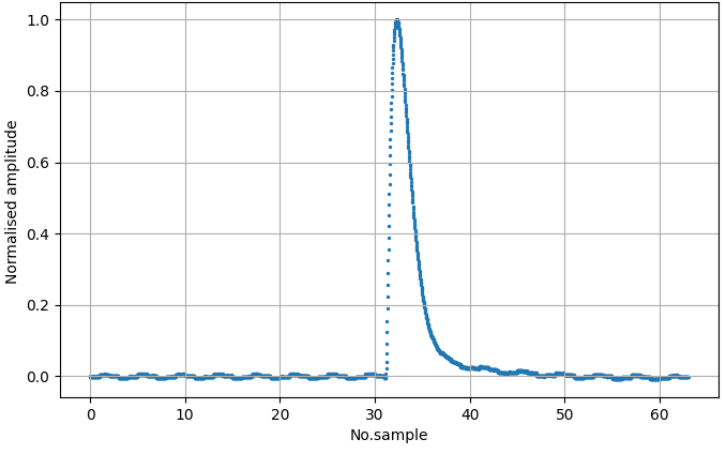

Fig. 3: Interpolated pulse shape from series of phase shifted measurements

FLAME pulse shape

Once the detailed pulse shape was obtained, the theoretical CR-RC response was fitted for the unit step function. As can be seen, the theoretical function matches with the shape obtained.

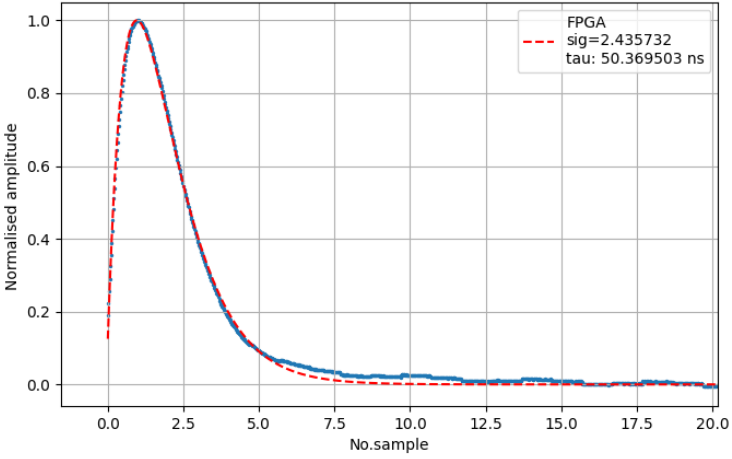

Fig. 4: Interpolated pulse shape from series of phase shifted measurements with CR-RC pulse fitted

FLAME readout linearity

In order to check the linearity of FLAME readout, charge was injected into one channel in range 4-250 fC. We can observe perfect linearity (R^2=0.9999) up to 180 fC.

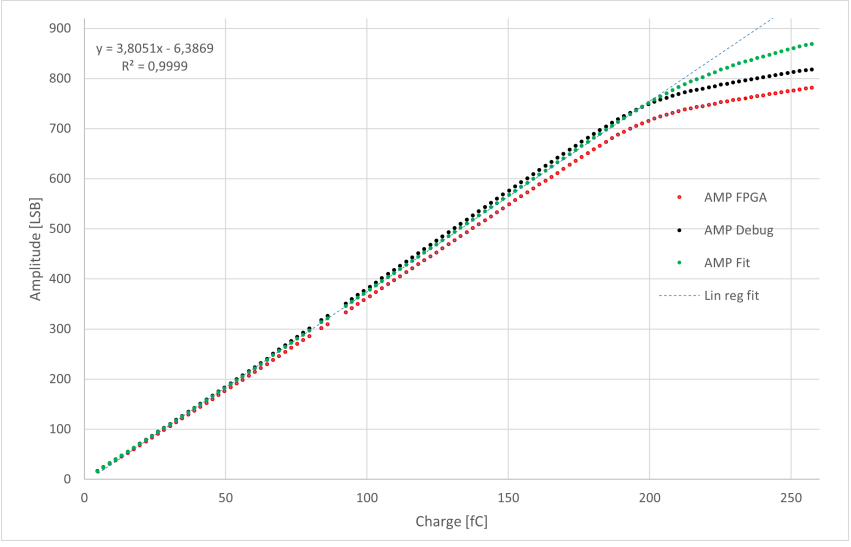

Fig. 5: FLAME readout response

Further measurements in progress...

Test-beam data analysis

Amplitude reconstruction

- FPGA - online reconstruction using deconvolution
- Debug - offline reconstruction from raw ADC data using deconvolution with corrected shaping time
- FIT - offline reconstruction from raw ADC data using fitting

Offline deconvolution from debug and fit to debug data give similar results.

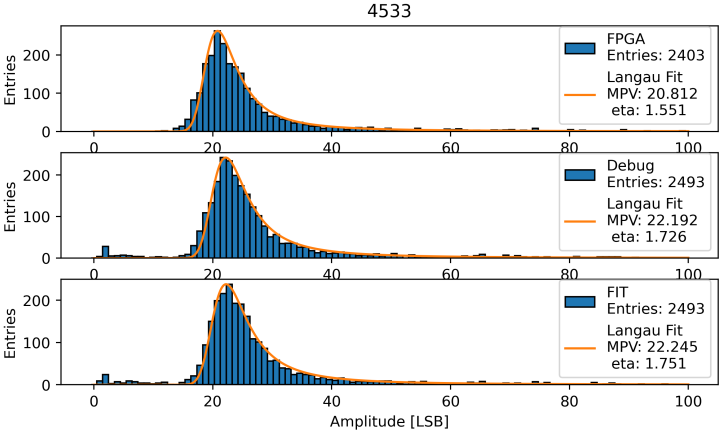

Fig. 6: Example of amplitude reconstruction histogram for run 4533

Time of arrival reconstruction

For the first time we started to look at the TOA(time of arrival) reconstruction, but we are very far from reaching conclusions.

Time-of-arrival reconstruction during test beam, offline deconvolution from debug and fit to debug data gives us also similar results.

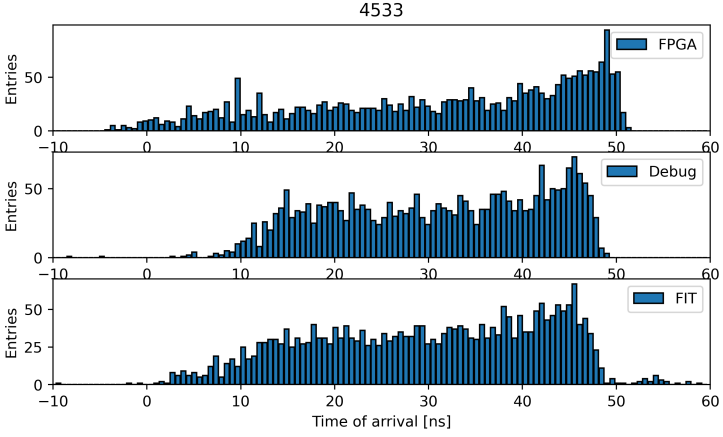

Fig. 7: Comparison of TOA reconstruction from deconvolution on FPGA, deconvolution from debug data and CR-RC FIT to raw ADC samples

MPV distribution in channels and sensors

Depending on the sensor MPV change from 19.93 to 21.41 LSB.

Several sensors were used during the test beam, and knowing the MPV position calibration can be performed.

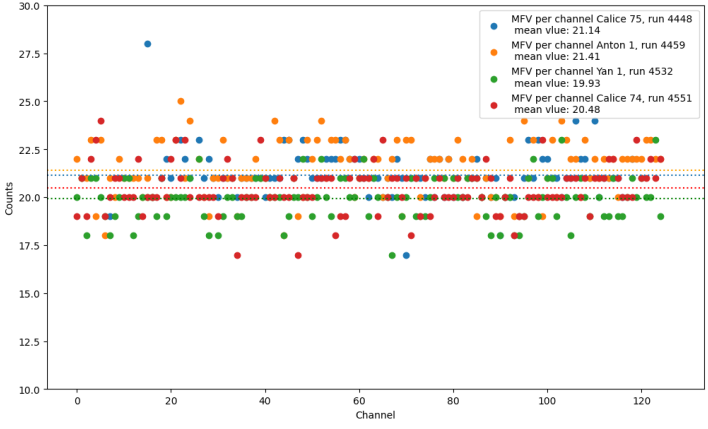

Fig. 8: MPV distribution in channels and sensors

Normalised MPV distribution in channels and sensors

Gain fluctuations are higher than those obtained in laboratory measurements. After normalisation by dividing by mean MPV per sensor we achieved correction factor for every channel and sensor.

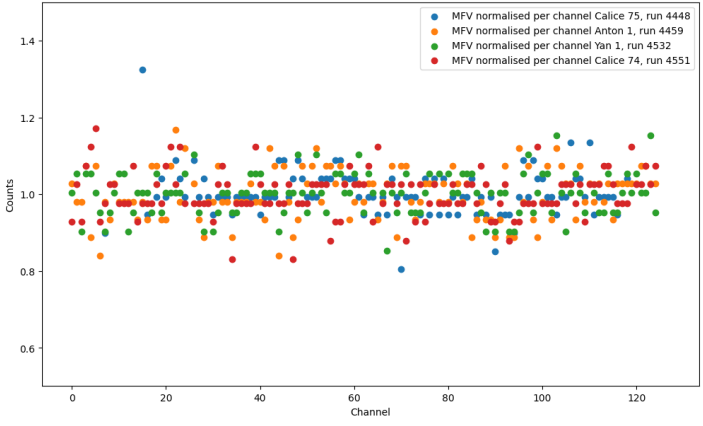

Fig. 9: Normalised MPV distribution in channels and sensors

Analysis of geometry

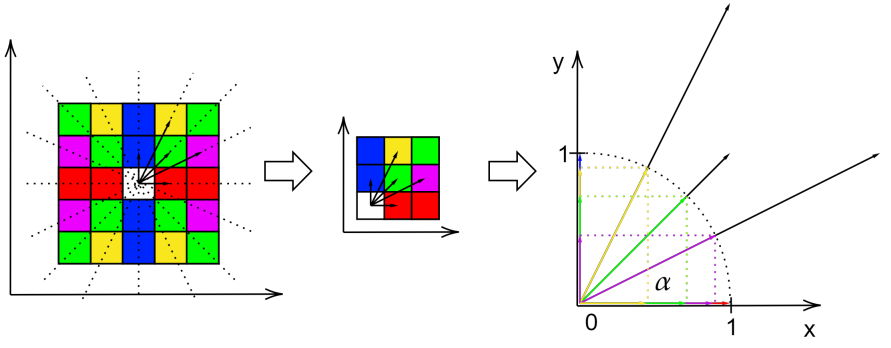

x	y	α
1	0	0
$\frac{2}{\sqrt{5}}$	$\frac{1}{\sqrt{5}}$	33
$\frac{1}{\sqrt{2}}$	$\frac{1}{\sqrt{2}}$	45
$\frac{1}{\sqrt{5}}$	$\frac{2}{\sqrt{5}}$	66
0	1	90

Fig. 10: Geometry explanation

Analysis of spatial configurations of 2-hit events

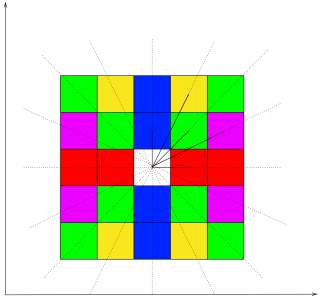

Fig. 11: Pad geometry

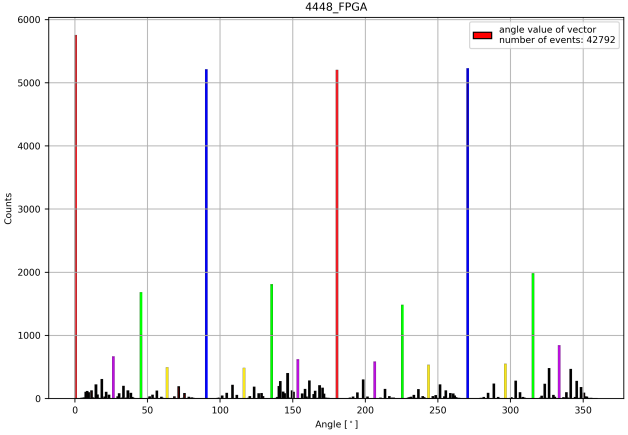

Fig. 12: Calice 75 run 4448

Analysis of hits geometry

Two ways to display information about angle

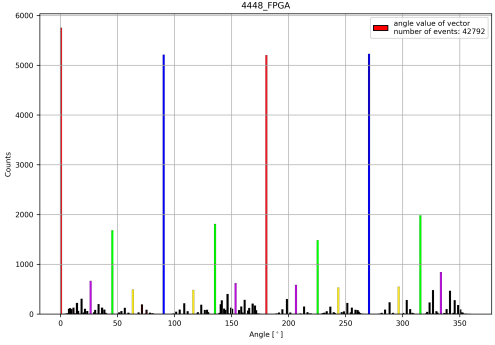

Fig. 13: Calice 75 run 4448

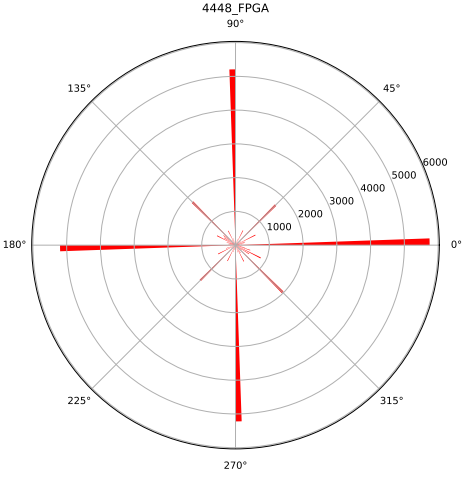

Fig. 14: Calice 75 run 4448

Anisotropy

In GaAs sensors, we can clearly see the anisotropy on the y axis - axis of trace direction.

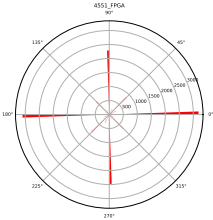

(a) Calice 74

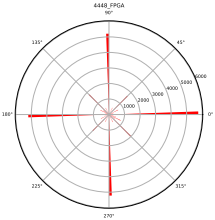

(b) Calice 75

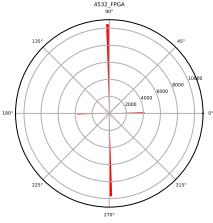

(c) Yan 1

(d) Anton 1

Amplitude of 2 hits events

In Anton 1 and Yan 1 sensors there are clearly visible differences in sum of amplitudes in event. Does big fraction of one particle 2-hit events come from:

- charge sharing?
- cross-talk?

To make firm conclusions we need to take in to account telescope data in our analysis.

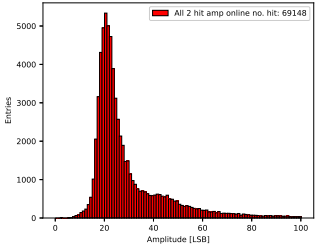

(a) Calice 74

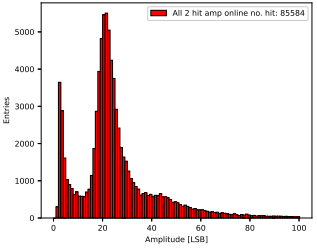

(b) Calice 75

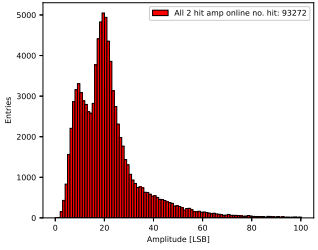

(c) Yan 1

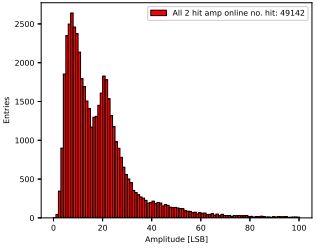

(d) Anton 1

Separation of 2-hit events types

In Anton 1 and Yan 1 sensors there are clearly visible differences in sum of amplitudes in event. Does big fraction of one particle 2-hit events come from:

- charge sharing?
- cross-talk?

How can we explain this distribution?

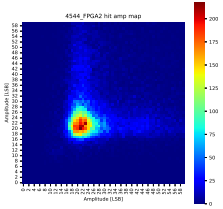

(a) Calice 74

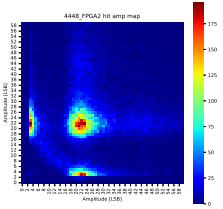

(b) Calice 75

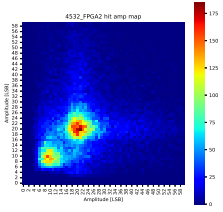

(c) Yan 1

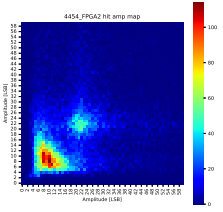

(d) Anton 1

Amplitude of 2 hits events

By making this separation, we are trying to observe 1-particle events and 2-particle events in 2-hit events.

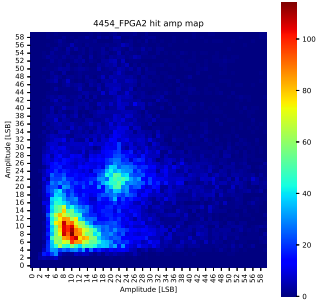

Fig. 18: Anton 1 run 4454

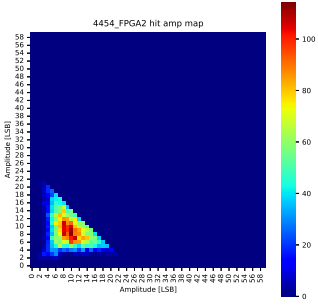

Fig. 19: Anton 1 run 4454 amplitude sum below 25

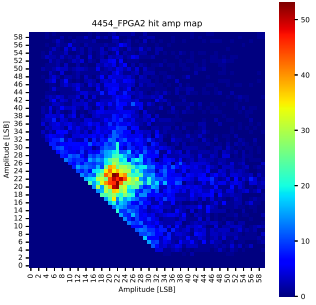

Fig. 20: Anton 1 run 4454 amplitude sum above 35

Angle after separation Yan 1

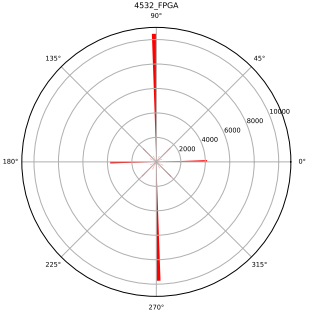

Fig. 21: Yan 1 run 4532

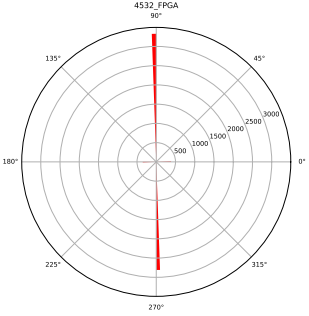

Fig. 22: Yan 1 run 4532 amplitude sum below 25

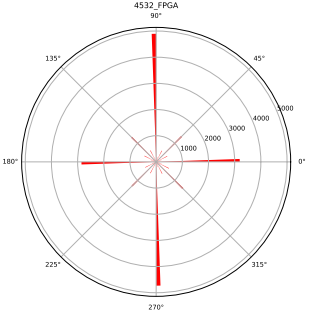

Fig. 23: Yan 1 run 4532 amplitude sum above 35

Baseline in time

An example of baseline over time for ch no. 0
BL value: 82.8 LSB

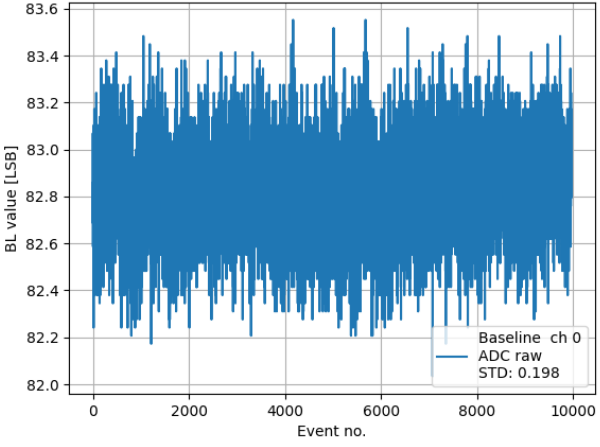

Fig. 24: Baseline value over time run 4533 10 000 events

Common-mode in time

Common-mode is not correlated with particular chip but appears globally in all channels.

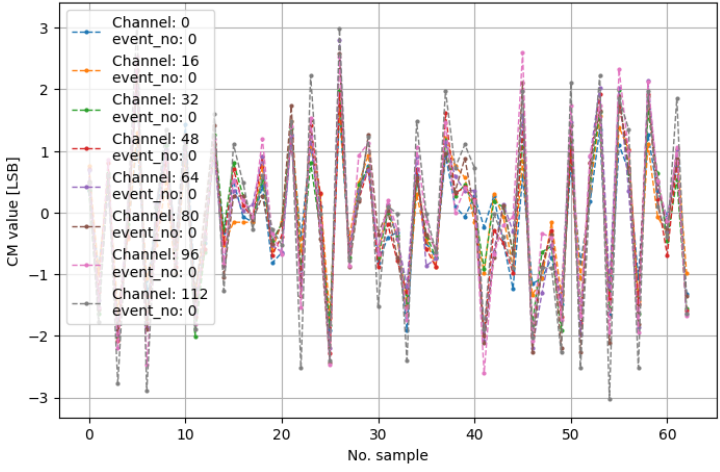

Fig. 25: Common-mode value in one event in run 4533

Common-mode in time

Using the discrete Fourier transform, we tested the common-mode for the existence of distinctive frequencies.

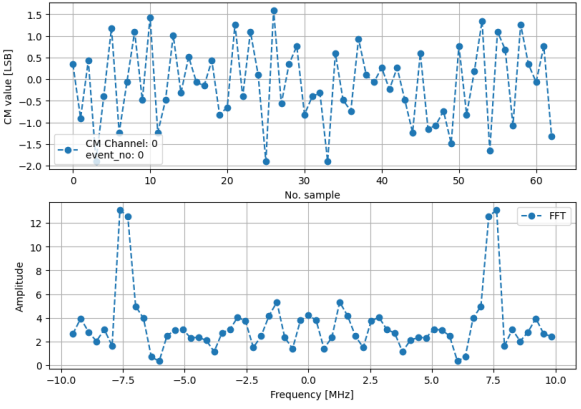

Fig. 26: Common-mode value and discrete Fourier transform in one event in run 4533

Common-mode in time

After summing the results of the Fourier transform of the 10 000 events, we can see that there is one distinct frequency: around 7 MHz.
In the lab commono-mode is much lower and without distinct frequency.

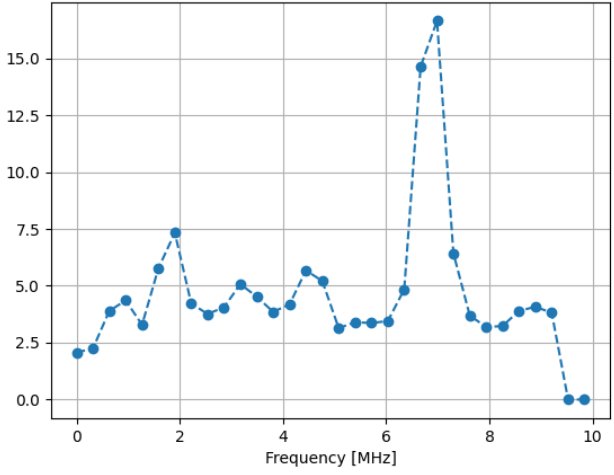

Fig. 27: Discrete Fourier transform of common-mode for 10000 events combined in run 4533

Deconvolution method

Deconvolution method

In our front-end we uses CR-RC shaping, for which amplitude response over time can be written as formula below:

$$V(t) = \frac{q_{in}}{C_{feed}} \frac{t}{\tau_{sh}} e^{-\frac{t}{\tau_{sh}}} \quad (1)$$

If we include time before pulse, non-zero pulse start time t_0, amplitude α and pedestal b, equation 1 is transformed into:

$$V(t) = \begin{cases} b, & \text{for } t < t_0. \\ \alpha \left(\frac{t-t_0}{\tau_{sh}} \right) e^{-\frac{t-t_0}{\tau_{sh}}} + b, & \text{for } t \geq t_0. \end{cases} \quad (2)$$

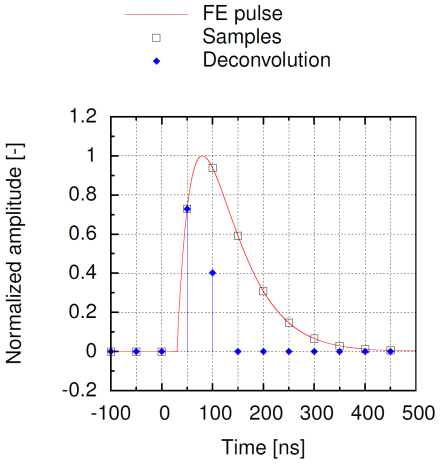

Fig. 28: Example of asynchronous sampling with two nonzero filter output samples at $t_0 = 30$ ns

Deconvolution method

Our output pulses are a convolution of its impulse response with the sensor's current signal (deposited charge), in order to find the input signal, we can use a procedure inverse to the convolution called deconvolution. In our system, this procedure is performed digitally by a digital filter. Output sample s_k of simplest FIR(Finite Impulse Response):

$$s_k = \sum_{i=0}^{N-1} w_i v_{k-i} \qquad (3)$$

w_i - weight associated with input sample v_{k-i}

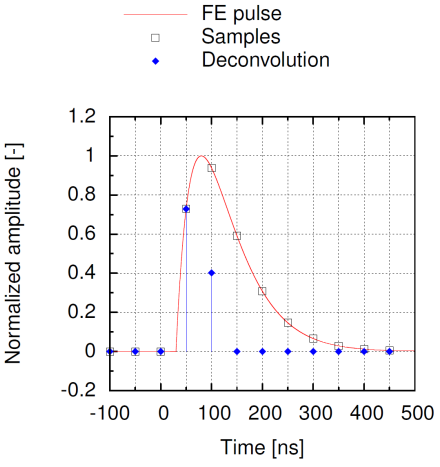

Fig. 29: Example of asynchronous sampling with two nonzero filter output samples at $t_0 = 30$ ns

Deconvolution method

To calculate amplitude of pulse we have to use some mathematical tools. Let start from front-end response $V_{sh}(s)$ in a Laplace domian can be expresed as:

$$V_{sh}(s) = \frac{1}{s} H(s) = \frac{1}{\tau_{sh}} \frac{1}{\left(s + \frac{1}{\tau_{sh}}\right)^2} \qquad (4)$$

$H(s)$ - transform function of the CR-RC shaper.

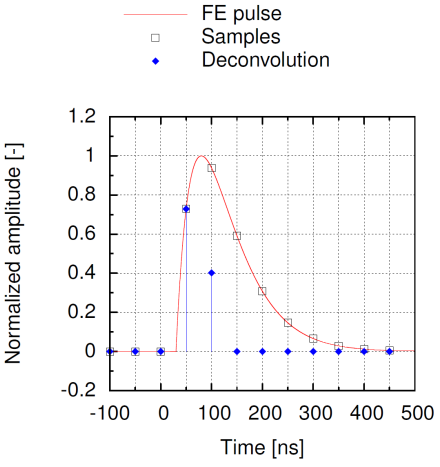

Fig. 30: Example of asynchronous sampling with two nonzero filter output samples at $t_0 = 30$ ns

Deconvolution method

Next step is to transform from continuous domain s to the discrete domain z using the Z transform. After that and we achieved discrete transform function $D(z)$:

$$D(z) = z^2 - 2e^{-\frac{T_{smp}}{\tau_{sh}}} z + e^{-\frac{2T_{smp}}{\tau_{sh}}} \quad (5)$$

Since z^2 represents the sample which will be received after 2 sampling periods, we can just multiplied by z^{-2} delaying all samples by two periods.

$$D(z) = 1 - 2e^{-\frac{T_{smp}}{\tau_{sh}}} z^{-1} + e^{-\frac{2T_{smp}}{\tau_{sh}}} z^{-2} \quad (6)$$

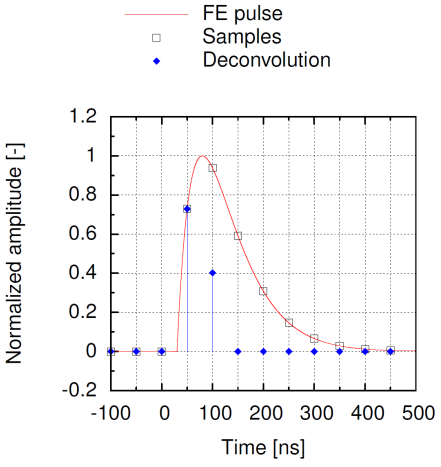

Fig. 31: Example of asynchronous sampling with two nonzero filter output samples at $t_0 = 30$ ns

Deconvolution method

Output sample value d_i, obtained at time $i \cdot T_{smp}$ can be expressed as:

$$d_i = v_i - 2e^{-\frac{T_{smp}}{\tau_{sh}}} v_{i-1} + e^{-\frac{2T_{smp}}{\tau_{sh}}} v_{i-2} \qquad (7)$$

where v_i is the shaper output:

$$v_i = V(i \cdot T_{smp}) \qquad (8)$$

If we calculate subsequent FIR output samples for CR-RC asynchronous shaper we can notice that filter produces only tow non zero samples or one in synchronous case.

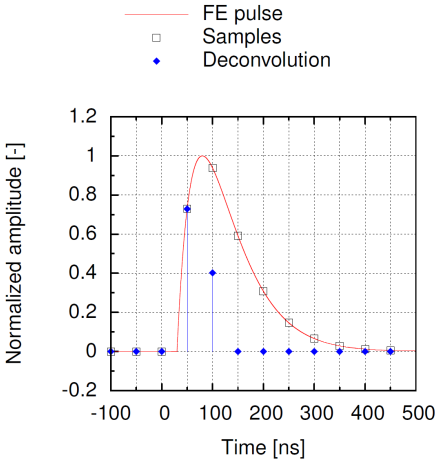

Fig. 32: Example of asynchronous sampling with two nonzero filter output samples at $t_0 = 30$ ns

Deconvolution method

Ratio between tow non-zero filter samples after reduction is given by:

$$\frac{d_2}{d_1} = \frac{t_0}{T_{smp} - t_0} e^{-\frac{T_{smp}}{\tau_{sh}}} \quad (9)$$

This ratio enable to calculate pulse starting time (TOA) which is necessary for amplitude reconstruction.

$$t_0 = \frac{\frac{d_2}{d_1} T_{smp}}{\frac{d_2}{d_1} + e^{-\frac{T_{smp}}{\tau_{sh}}}} \quad (10)$$

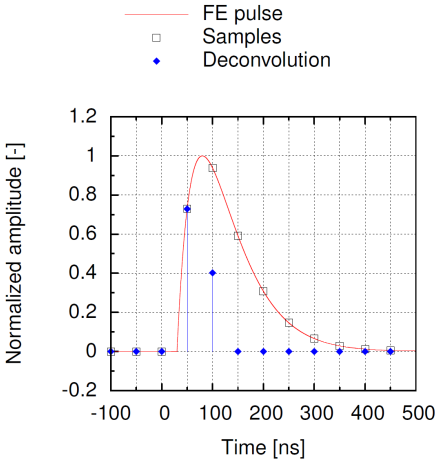

Fig. 33: Example of asynchronous sampling with two nonzero filter output samples at $t_0 = 30$ ns

Deconvolution method

Sum of two non-zero filter samples after reduction can be expressed as:

$$d_1+d_2 = \frac{A}{\tau_{sh}} e^{-\frac{T_{smp}-t_0-\tau_{sh}}{\tau_{sh}}} \left[T_{smp} - t_0 \left(1 - e^{-\frac{T_{smp}}{\tau_{sh}}} \right) \right] \tag{11}$$

This sum enable to calculate pulse amplitude A

$$A = (d_1 + d_2) \left[\frac{\tau_{sh}}{T_{smp}} e^{\frac{T_{smp}-\tau_{sh}}{\tau_{sh}}} \right] \frac{e^{\frac{-t_0}{\tau_{sh}}}}{1 - \frac{t_0}{T_{smp}} \left(1 - e^{-\frac{T_{smp}}{\tau_{sh}}} \right)} \tag{12}$$

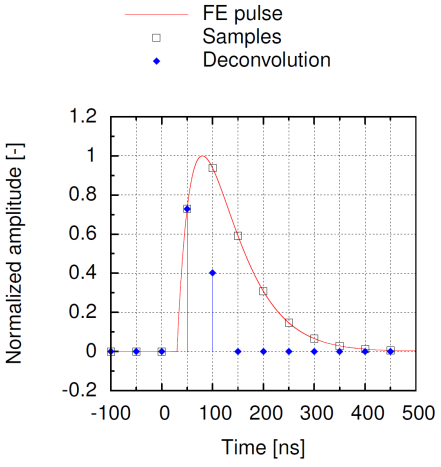

Fig. 34: Example of asynchronous sampling with two nonzero filter output samples at $t_0 = 30$ ns

Deconvolution method

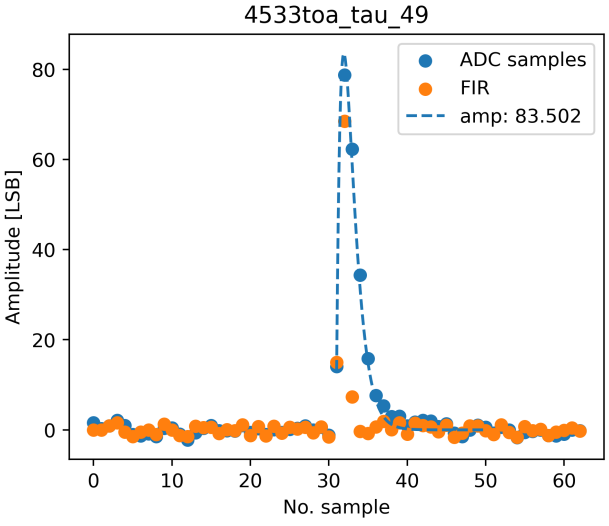

Fig. 35: Result of deconvolution method on data from run 4533

Thank you for attention

Amplitude vs time of arrival

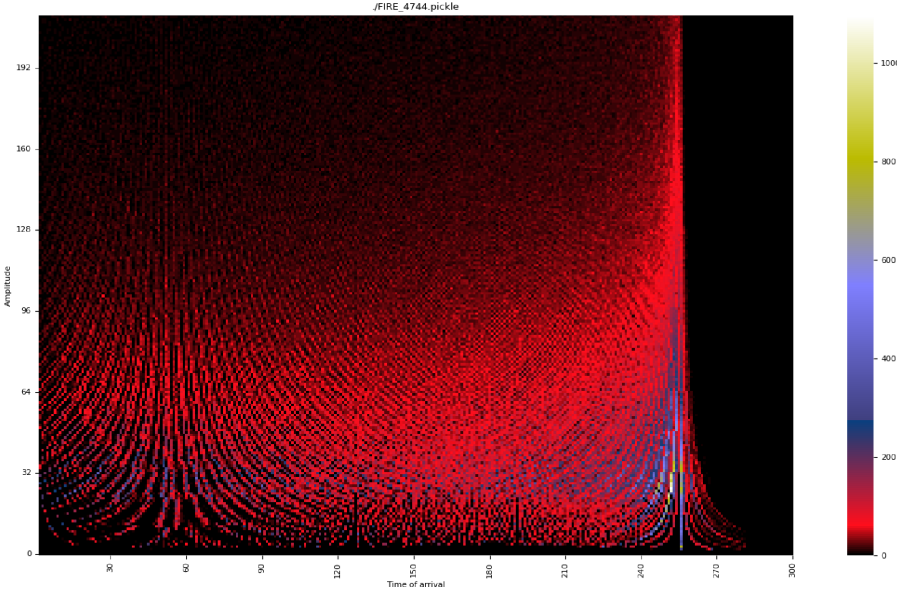

Fig. 36: Interesting dependency between amplitude and TOA